FORMATION OF AMORPHOUS METAL BY HYPERVELOCITY IMPACT

M. L. Spann and L. D. Brown

Presented at the
International Conference on Metallurgical Castings
(Sponsored by Vaccum Metallurgy Division American Vacuum Society)
(See RF-38)

Publication No. PR-12
Center for Electromechanics
The University of Texas at Austin
Balcones Research Center
EME 1.100, Building 133
Austin, TX 78758-4497
(512)471-4496

PR-12

FORMATION OF AMORPHOUS METAL BY HYPERVELOCITY IMPACT

M. L. Spann and L. D. Brown
Center for Electromechanics
The University of Texas at Austin
Austin, TX 78712

ABSTRACT

The Center for Electromechanics at The University of Texas at Austin has investigated the use of an electromagnetic railgun accelerator for the deposition of non-crystalline metals. The two main objectives of the study were to produce non-crystalline metal deposits in single thin layers (~ 25 μm thick) and to determine the feasibility of building thicker layers by making multiple deposits.

Deposits have been analyzed using a variety of techniques, including electrical resistivity and resistivity ratio, x-ray diffraction, and transmission electron microscopy. Differential scanning calorimetry was carried out at Battelle Columbus Laboratories. The measurements show that CEM-UT has produced non-crystalline $Fe_{78}B_{13}Si_9$ deposits. Single- and multiple-layer non-crystalline deposits with thicknesses of up to 36 μm have been produced, and the upper thickness limit of the technique has not yet been determined.

INTRODUCTION

Metallic glasses introduce a new class of magnetic materials having a high resistivity relative to their magnetic crystalline counterparts. Such materials would be useful in making motors that are more efficient due to reduction in eddy current losses. Core losses are typically only 25 percent of the losses in M-4 electrical steel at 60 Hz in the 1.0-1.6 T region.(1)

The Center for Electromechanics at The University of Texas at Austin (CEM-UT), working under contract from the Electric Power Research Institute (EPRI), has investigated the formation of non-crystalline material by hypervelocity impact.

RAILGUN ACCELERATORS

Railguns are devices which can accelerate arc plasmas or solid projectiles by the interaction of currents and magnetic fields. The railgun designed and built for this project has a 1.27-cm (0.5-in.) square bore and is powered by a capacitor bank energy supply. A schematic drawing of the railgun concept is presented in Fig. 1.

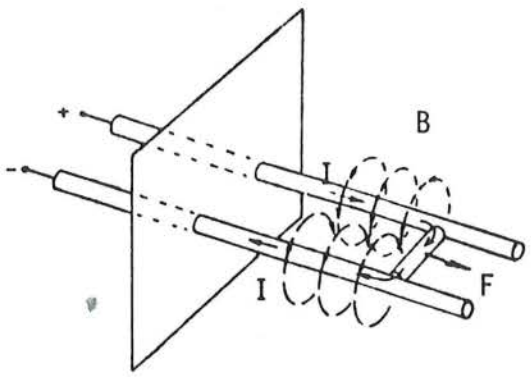

Figure 1. Railgun Concept

Current travels in opposite directions along parallel rails. The current path between the rails (usually an arc plasma) forms the armature and is accelerated by the Lorentz force:

$$F = 0.5\ L' I^2$$

where L' = rail inductance per unit length
I = current.

In general, L' is less than 0.5 μH/m, and large currents are necessary to induce appreciable forces. The CEM-UT/EPRI railgun energy store system is capable of providing currents in excess of 100 kA peak, which is sufficient to accelerate a 0.25-g (0.01-oz) projectile to velocities of 2 km/s. At approximately 1.6 km/s, the kinetic energy of an iron projectile is equivalent to the energy required to melt it.

All material loaded and fired was a single alloy and condition, viz., non-crystalline $Fe_{78}B_{13}Si_9$ (Metglas alloy 2605S2).

The arc was formed by a single layer of foil $Fe_{78}B_{13}Si_9$ wrapped around a ceramic block. The block was sized to be a tight fit in the bore and clamped the fuse against the rails. Additional material was cut into small pieces ~ 1.1 cm (0.43 in.) square and spot welded to the front of the fuse. Since the squares did not touch the rails, there was some degree of confidence that only the last layer, or fuse, formed the arc and accelerated the squares ahead of it. The leaf fuses investigated ranged from a single layer (the fuse) with no additional squares, ~ 100 mg, to a fuse with 20 squares attached, with a mass of 437 mg. Deposits made using this method ranged from 1 to 276 mg deposited, the most successful results being those with 20 to 30 mg.

The majority of the shots made were done with the chamber evacuated to a pressure of from 0.2 to 0.5 torr, and all successful shots were made in this pressure range.

Another variable investigated was the target temperature. While most shots were made at room temperature, it was considered desirable to cool

the target to increase the quench rate. Provisions were made to cool the target through the target end flange with liquid nitrogen while maintaining a vacuum in the chamber. This was tried and proved unsuccessful with copper targets. The copper targets were chilled to approximately 100 K, and shots were made over a range of conditions, including the mass loaded and the capacitor bank voltage, but the resulting deposits were unsatisfactory. They consisted of small, irregular-shaped regions of deposited material surrounded by a slight discoloration. It was apparent that only the highest-energy particles were adhering to the target, and that the majority of the particles were bouncing off. Copper had been a logical choice of target material for the low-temperature experiments, since it was readily available, has a high thermal conductivity, and had been used successfully as a room-temperature target material. It was later suggested that the high thermal conductivity was causing the lack of adhesion at low temperature by conducting the heat away from the surface before local melting and bonding of the deposit material to the target could occur. Very late in the program, shots were made using stainless steel targets at 100 K which were shown by subsequent tests to have been the most successful shots made during the project.

SPECIMEN EVALUATION

We could find no single definitive test for determining the non-crystallinity of a specimen. Therefore, several test methods were used. The first of these methods was measurement of resistivity and resistivity ratio. The resistivity ratio is the ratio of the resistance measured at room temperature (~ 300 K) to the resistance of the same specimen measured at liquid nitrogen temperature (77 K). Typical resistivity ratio measurements made using the four-probe and Van der Paw techniques (3) are given in Table 1.

The most successful deposits were made under the following conditions:

Bank capacitance	350 μF
System inductance	2.3 μH
Bank voltage	7 - 8 kV
Peak current	72 - 85 kA
Charge type	leaf foil fuse
Charge mass	~ 160 mg
Deposited mass	20 - 30 mg
Target material and temperature	Cu at room temperature or Stainless steel at 100 K

The deposits that had passed the visual examination were then characterized as to the presence or absence of crystallinity using x-ray diffraction (XRD), transmission electron microscopy (TEM), electrical resistivity, and differential scanning calorimetry (DSC). Because of the time-consuming nature of most of these tests, the deposits were first screened using the simplest technique, XRD. Those samples which were shown to be largely non-crystalline by the absence of any sharp, well-defined diffraction peak above the broad amorphous reflection were studied further by the other techniques.

Table 1

RESISTIVITY AND RESISTIVITY RATIO MEASUREMENTS

Specimen	Four-probe Technique ρ, μΩ-cm	Four-probe Technique ρ_{RT}/ρ_{LN_2}	Van der Paw Technique ρ, μΩ-cm	Van der Paw Technique ρ_{RT}/ρ_{LN_2}	Structure
Metglas strip					
As-received	125	1.03	200	1.01	NC
450 C/8 hr ann.	111	1.01	247	1.04	<0.01 μm nuclei
450 C/50 hr ann.	--	--	93	1.03	<0.01 μm nuclei
Railgun deposits					
Shot No. 21	--	--	375	0.95	<500 Å grain size
Shot No. 28	--	--	190	1.04	NC/C

NC = Non-crystalline; C = Crystalline

To make a proper four-point probe measurement on the railgun deposited material would require removal of an intact 1 x 10-mm (0.04 x 0.39-in.) specimen from the target. This was generally not possible, due to the tenacity of the deposit-target bonding and the porosity of the deposit. Therefore, the Van der Paw method was used, which does not require such well-defined specimen geometry.

While the resistivity ratio may give a good indication of non-crystallinity, it was not well-suited for evaluating the specimens generated during this project. One reason was the difficulty in removing the deposits from the substrates. In many cases, this could not be accomplished without destroying the deposits. On samples that could be tested, the resistivity ratio was not very reliable. Sample 21, known to be crystalline with 500-Å crystals, had a lower resistivity ratio than the as-received Metglas, while Sample 28, which was largely non-crystalline, had the same resistivity ratio as the crystallized Metglas samples. The unsatisfactory resistivity ratio results are believed to be due to the small sizes and nonuniform cross sections of

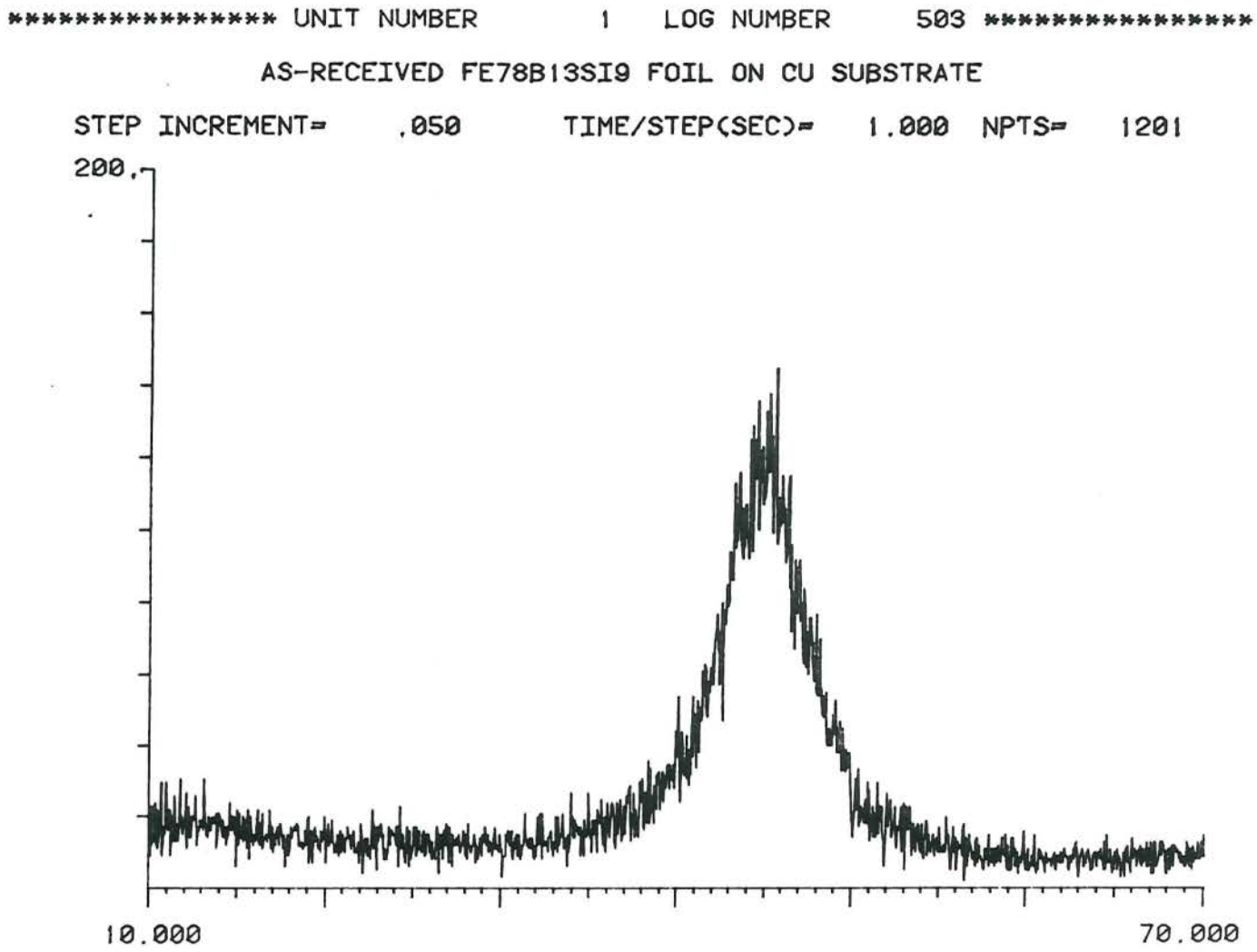

Fig. 2. X-ray Diffraction Pattern from As-received Metglas

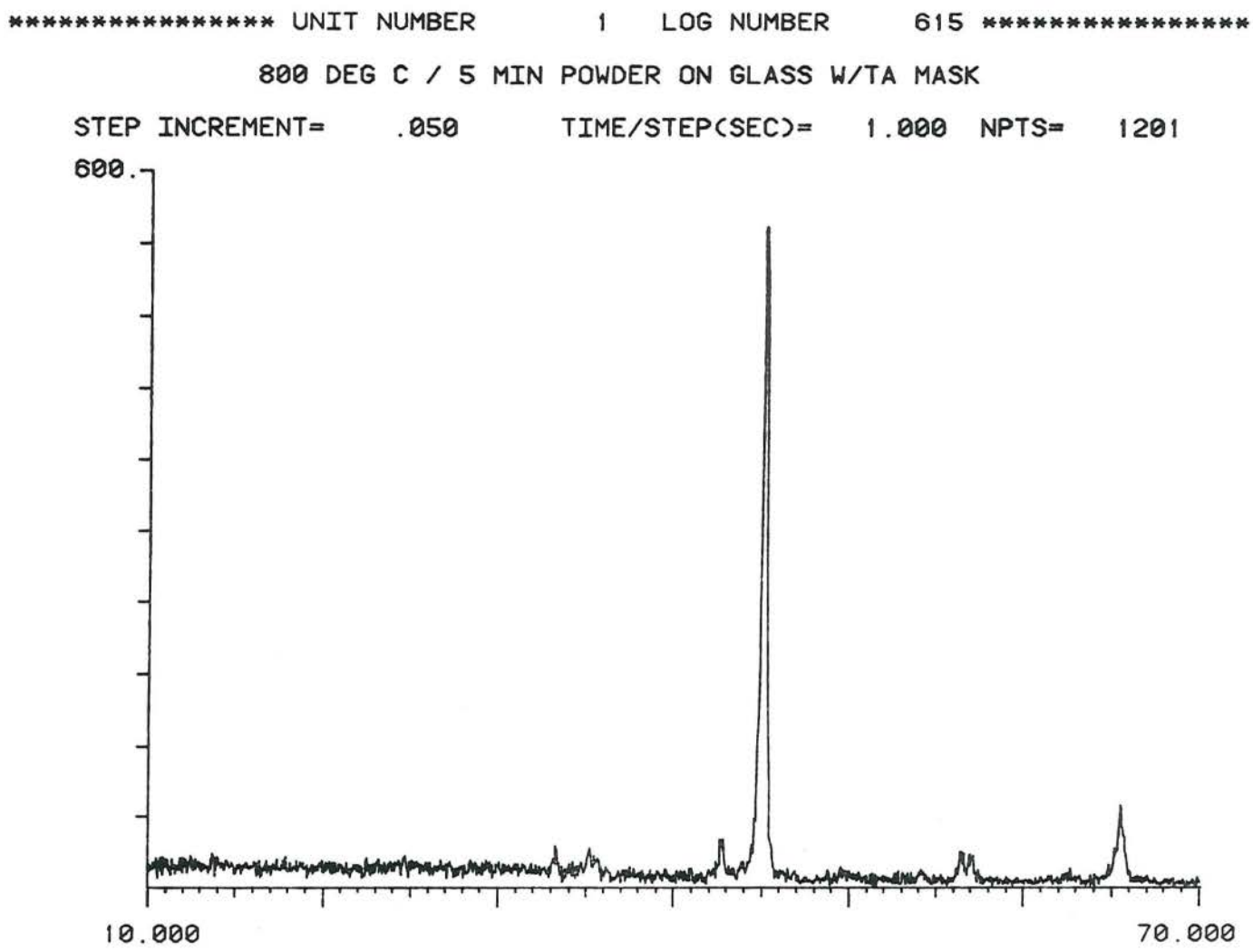

Fig. 3. X-ray Diffraction Pattern from Annealed Metglas

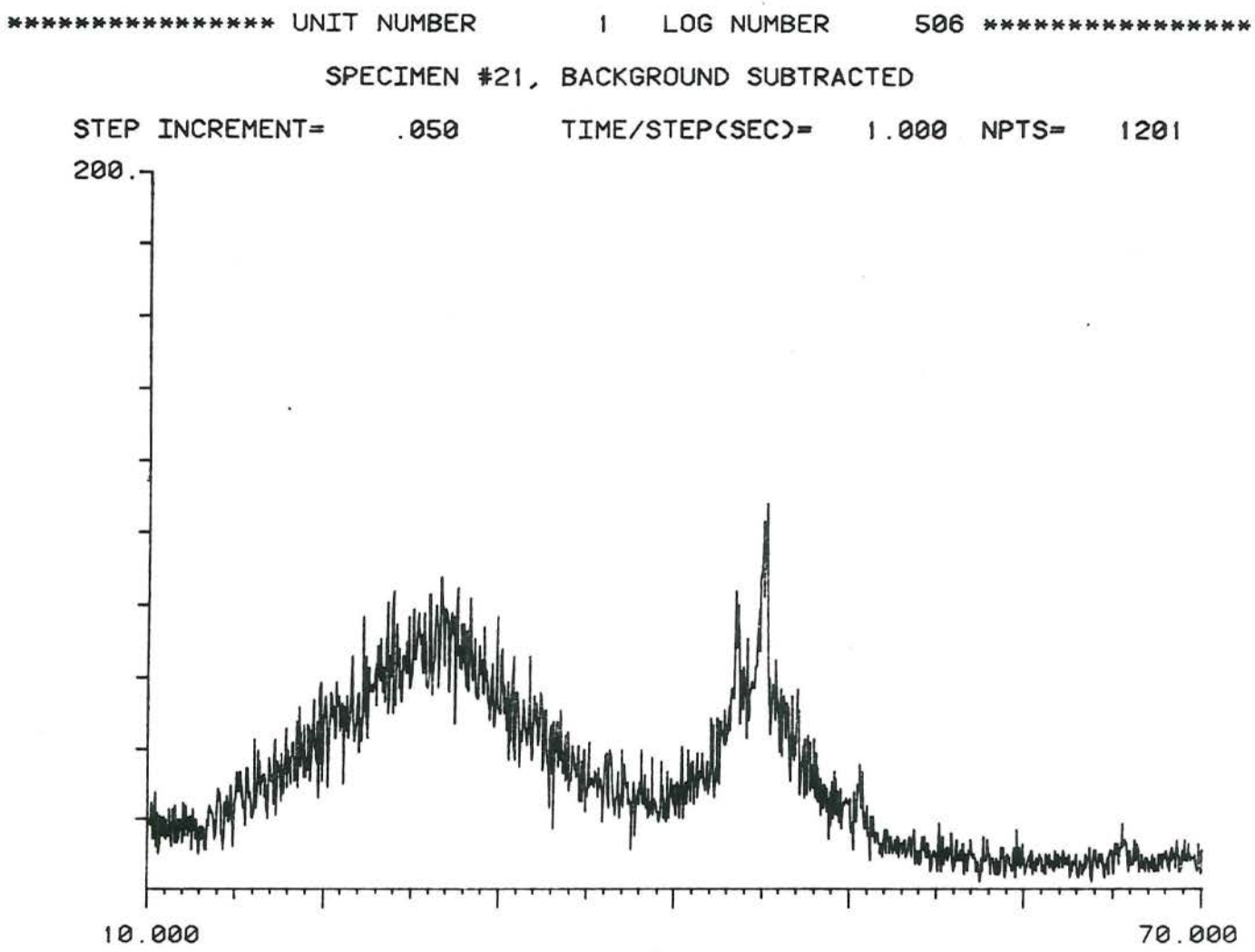

Fig. 4. X-ray Diffraction Pattern from Specimen 21
Broad peak at 27 degrees is from a
carbonaceous contaminant.

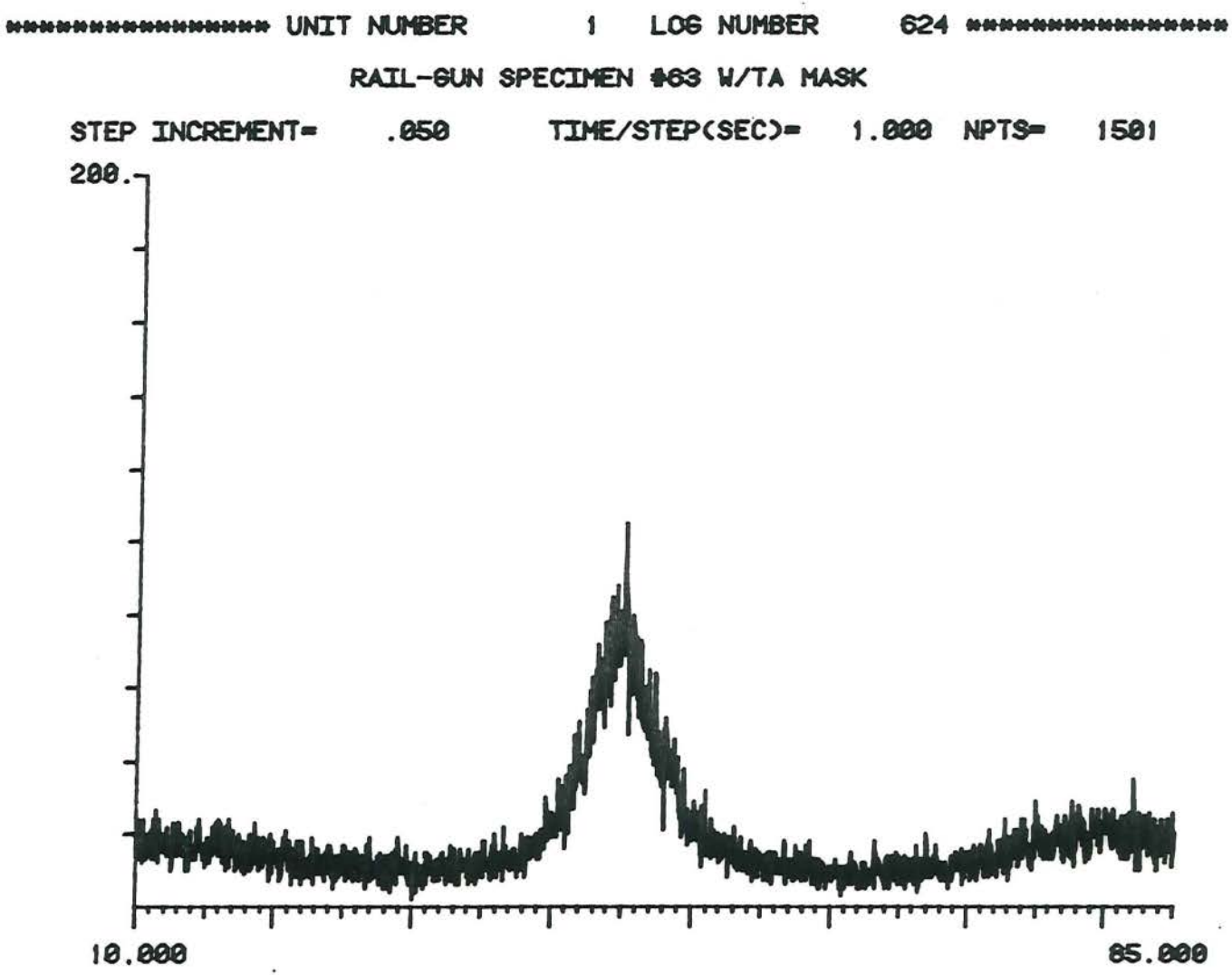

Fig. 5. X-ray Diffraction Pattern from Specimen 63

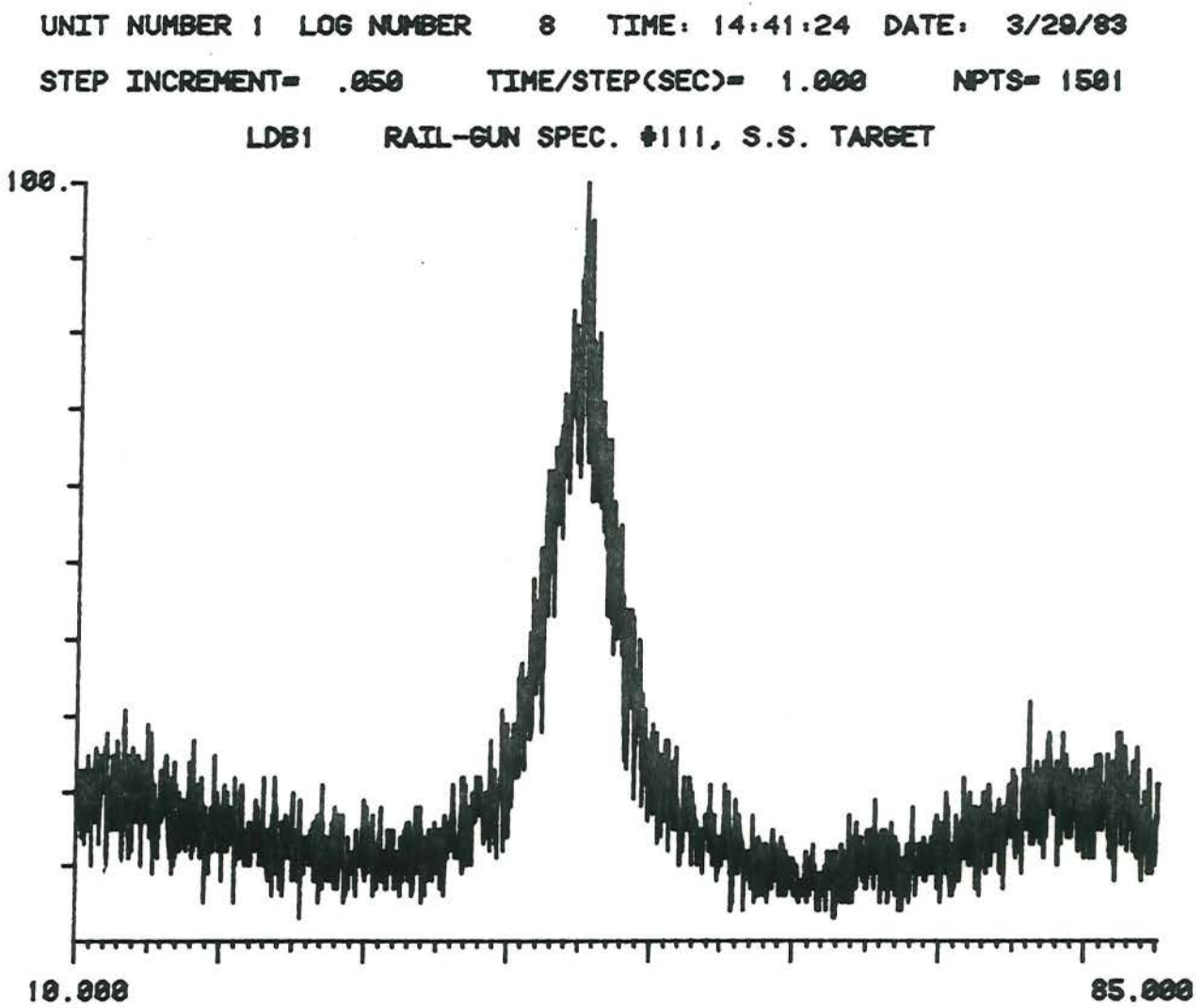

Fig. 6. X-ray Diffraction Pattern from Specimen 111

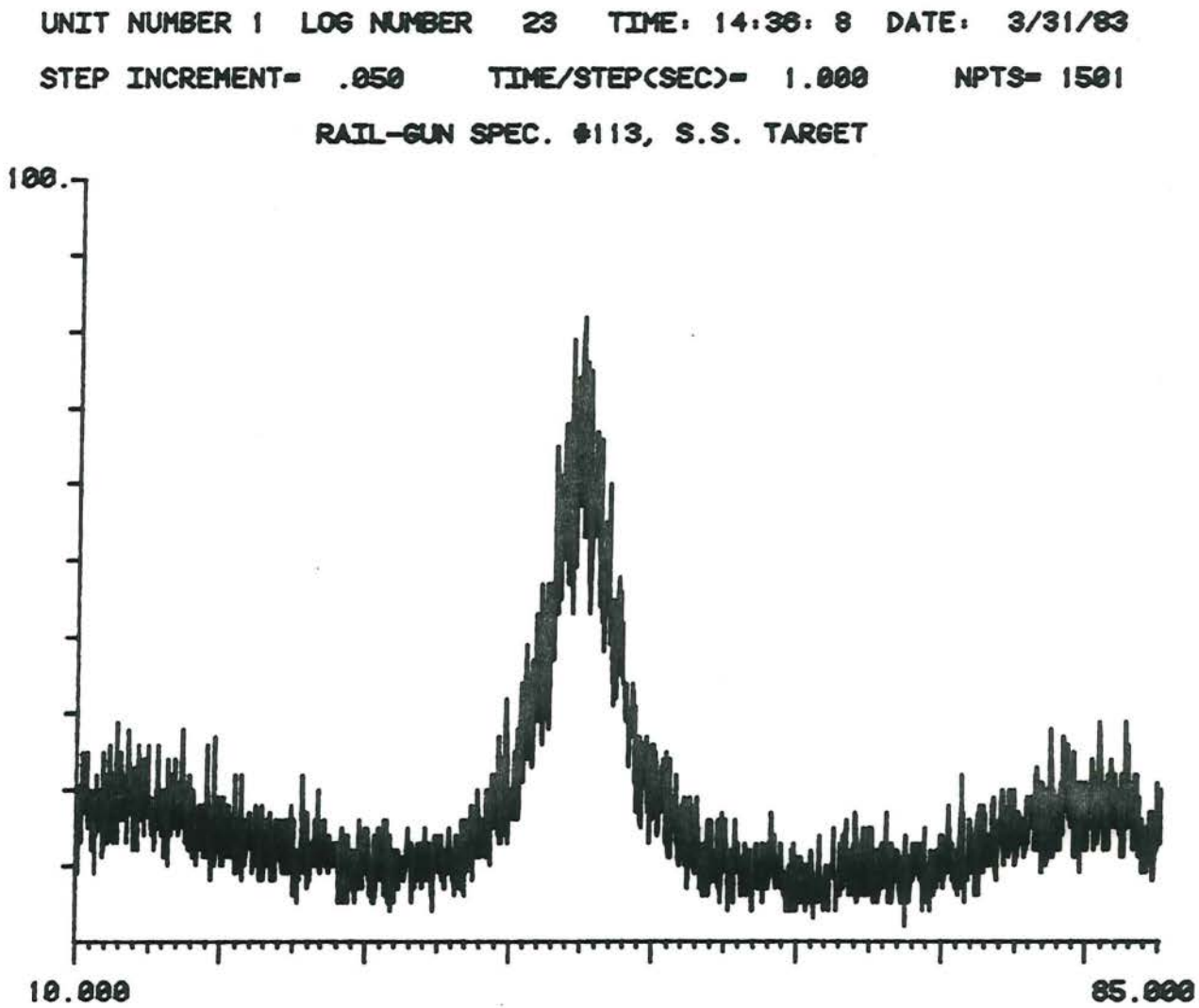

Fig. 7. X-ray Diffraction Pattern from Specimen 113

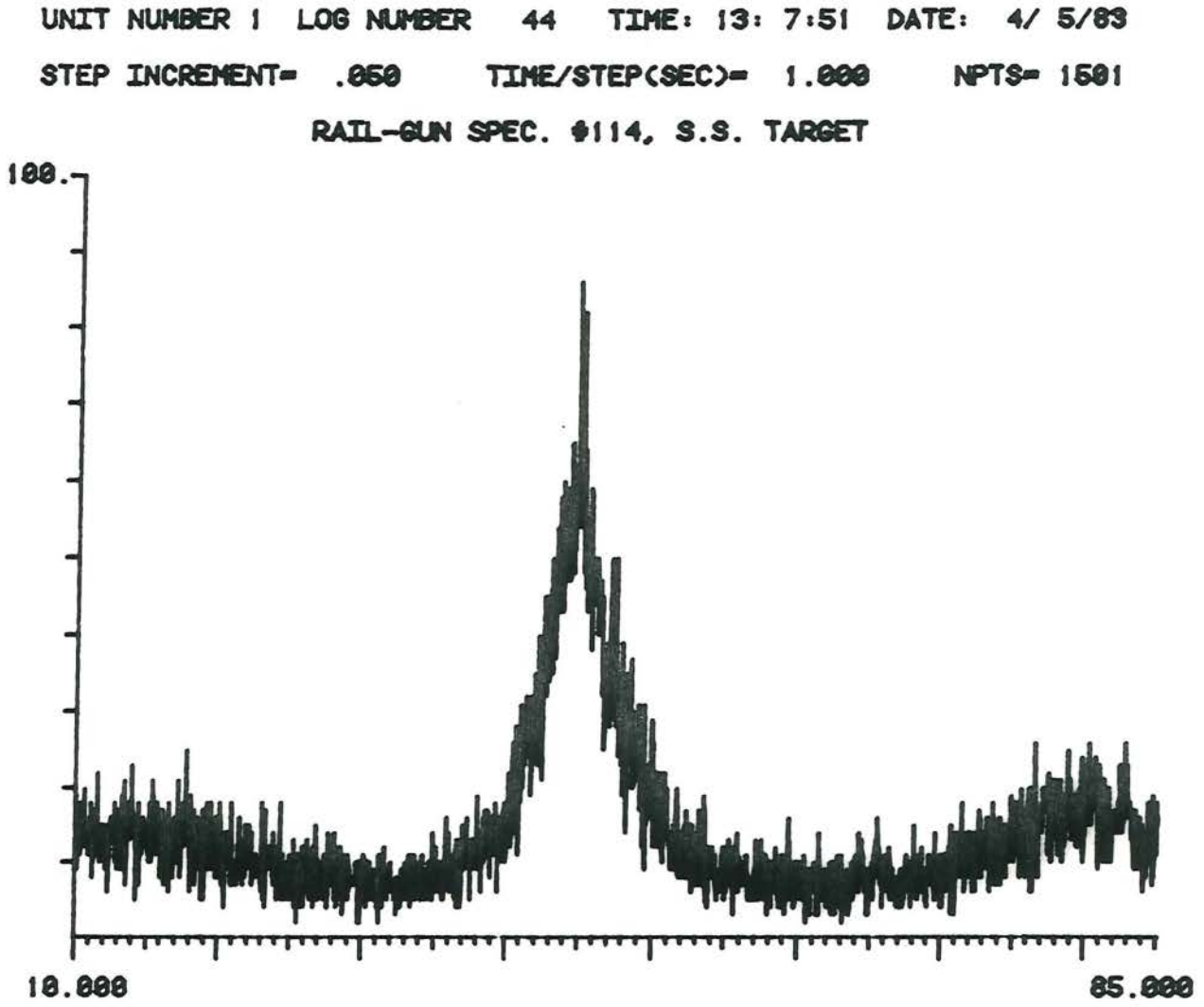

Fig. 8. X-ray Diffraction Pattern from Specimen 114

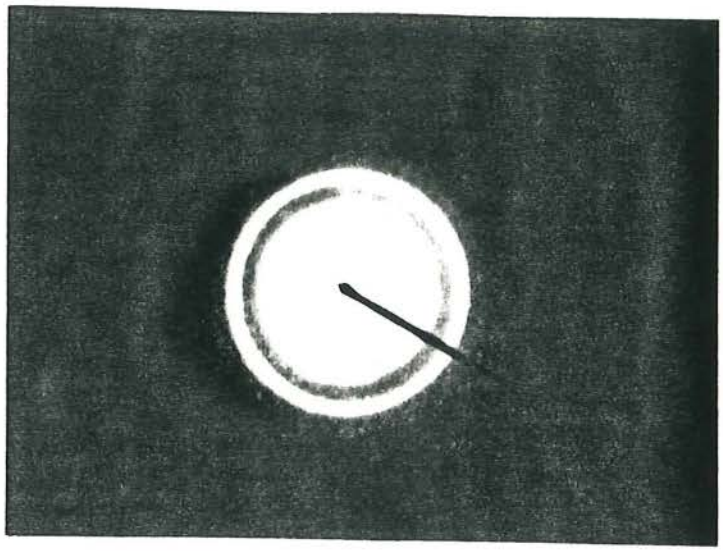

Fig. 9. Electron Diffraction Pattern
from As-received Metglas

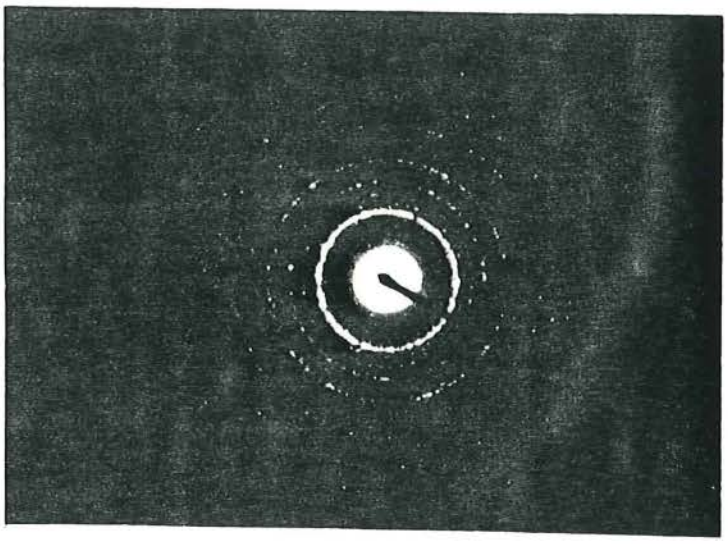

Fig. 10. Electron Diffraction Pattern
from Annealed Metglas

Fig. 11. TEM Micrograph of Specimen 21
200,000 X

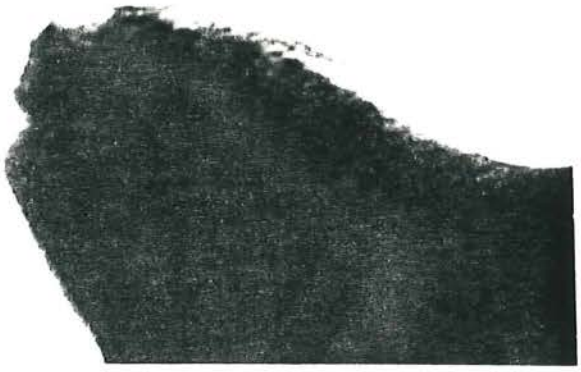

Fig. 12. TEM Micrograph of Unthinned
Specimen 28 400,000 X

the samples. Because of the difficulties encountered and the inconsistent results obtained with resistivity ratios, effort was concentrated on development of the x-ray diffraction method.

The non-crystalline material has a broad, diffuse peak (Fig. 2), while the crystalline material shows a narrow, well-defined peak at 45° 2θ (Fig. 3). Partially crystalline material has a pattern which is a combination of these two, an example of which is the pattern for Specimen 21 presented as Fig. 4.

X-ray diffraction patterns for Specimens 63, 111, 113, and 114 are presented in Figs. 5 through 8. The XRD patterns are very similar to that of the as-received foil. A very small amount of crystallinity is apparent in the patterns from Specimens 63 and 114, however. TEM studies of Specimen 63 found all non-crystalline material. A differential scanning calorimeter (DSC) study performed by Battelle Columbus Laboratories judged Specimen 63 to be 85-86 percent non-crystalline. On the basis of these tests, we believe that Specimens 111 and 113 were essentially non-crystalline (95 percent or greater).

Specimens 111, 113, and 114 were all deposits on chilled (100 K) stainless steel targets which could not be removed for TEM examination. It is interesting that Specimen 113, a three-layer deposit, and Specimen 114, a five-layer deposit, show little or no signs of crystallinity, suggesting that non-crystalline deposits with even larger numbers of layers are possible on chilled stainless steel.

Transmission electron microscopy was the basic method used to test samples which could be removed from the targets. The electron diffraction pattern for the as-received Metglas is presented in Fig. 9. Corresponding data for crystallized Metglas is shown in Fig. 10. The differences are readily apparent in the well-defined rings of the electron diffraction pattern and the visible crystals of the bright field micrograph in the crystalline material.

Figure 11 shows the grain structure of Specimen 21. The grains have an average diameter of 500 Å. No non-crystalline material was present in any of the TEM samples prepared from this specimen.

Specimen 28 was studied both unthinned and thinned. This specimen was almost entirely non-crystalline. In unthinned edges of one sample, there were a few areas which were largely non-crystalline, but which contained a grain or two of crystalline material measuring about 250 Å in diameter (Fig. 12). The corresponding diffraction pattern is difficult to index because of its incompleteness, but the crystalline phase appears to have been α-Fe. When entire samples from Specimen 28 were thinned, however, they invariably were entirely non-crystalline.

The likely explanation for the differing results is that very small crystalline regions originally present at or near the air side of the deposit were preferentially dissolved before thinning of the non-crystalline material was complete. This explanation is consistent with the observation that in thinning non-crystalline and crystallized

Metglas foil, the crystallized specimens always thinned faster. This also explains the small crystalline peak often found in the XRD patterns.

The Center for Electromechanics has successfully produced non-crystalline material in both single-layer and multiple-layer railgun deposits. The best results were obtained using chilled stainless steel substrates. The upper limit of non-crystalline deposit thickness that can be achieved has not been determined. A summary of the results is presented in Table 2.

Table 2

SUMMARY OF RESULTS

Shot No.	No. of Layers	Tgt. Matl.	Temp. (K)	Bank Voltage (kV)	Peak Current (kA)	Deposit Mass (g)	Character-ization	Analy-tical Methods
3	1	Cu	297	5	51	n.a.	C-0.2 μm	RR,TEM
21	"	"	"	6	95.9	0.051	C-500 Å	RR,XRD, TEM
28	"	"	"	7	70.0	0.025	largely NC-occ. 250 Å	RR,XRD, TEM
43	2	"	"	8	78.6; 78.1	0.049	largely NC	XRD
61	1	"	"	7	73.4	0.029	" "	XRD,TEM
63	1	"	"	7	72.6	0.030	NC	" "
111	1	SS	100	7.8	85.4	0.011	"	"
113	3	"	"	8; 7.8; 7.7	85.0; 84.3; 82.1	n.a.	"	"
114	5	"	"	7.8; 7.6; 7.5; 7.4; 7.4	84.0; 79.0; 78.8; 78.4; n.a.	0.042	"	"

NC - essentially non-crystalline; C - crystalline

CONCLUSIONS

The Center for Electromechanics has investigated the formation of non-crystalline material by hypervelocity impact. The goals of forming non-crystalline material in single- and multiple-layer deposits have been achieved. Multiple-layer deposits to a thickness of 36 μm have been produced, and the limit of the process has not been reached.

While this project was done using single-shot, slow-repetition-rate apparatus, technology exists for developing a high-repetition-rate system. Compensated pulsed alternators (4) are currently being designed that could drive a properly-fed railgun at a discharge rate of at least up to 200 Hz. Based on this technology, fabrication of thicker non-crystalline metal shapes and coatings appears to be possible.

REFERENCES

1. Allied Corp., "Metglas Electromagnetic Alloys," Brochure 15M-10/81.

2. Rashleigh, S. C., and Marshall, R. A., "Electromagnetic Acceleration of Macroparticles to High Velocities,", J. Appl. Phys. 49(4), Apr. 1978, 2540-2542.

3. Fisk, Z., and Webb, G. W., "Electrical Resistivity of Metals," in Treatise on Materials Science and Technology, Vol. 21, F. Y. Fradin, ed., Academic Press (New York), 1981.

4. Bird, W. L., et al., "The Compensated Pulsed Alternator Program -- A Review," IEEE Pulsed Power Conf., 3rd, Albuquerque, NM, June 1981.